



Published in final edited form as:

Biol Psychiatry. 2010 September 1; 68(5): 433–441. doi:10.1016/j.biopsych.2010.04.028.

Exaggerated and Disconnected Insular-Amygdalar BOLD Response to Threat-Related Emotional Faces in Women with Intimate-Partner Violence PTSD

Greg A. Fonzo¹, Alan N. Simmons^{2,3,5}, Steven R. Thorp^{2,3}, Sonya B. Norman^{2,3}, Martin P. Paulus^{2,3}, and Murray B. Stein^{2,3,4}

¹San Diego State University/University of California-San Diego Joint Doctoral Program in Clinical Psychology, San Diego, California

²Department of Psychiatry, University of California San Diego, La Jolla, California

³VA San Diego Healthcare System, San Diego, California

⁴Department of Family and Preventive Medicine, University of California San Diego, La Jolla, California

⁵Center of Excellence in Stress and Mental Health, San Diego, California

Abstract

Background—Imaging studies of posttraumatic stress disorder (PTSD) have identified functional differences in the amygdala and anterior cingulate (ACC)/medial prefrontal cortex during emotion processing. Recent investigations of the limbic sensory system and its associated neural substrate, the insular cortex, have demonstrated its importance for emotional awareness. Intimate-partner violence (IPV) is one of the most common causes of PTSD among women. This study examined the hypothesis that women with IPV-PTSD show a dysregulation of this limbic sensory system while processing threat-related emotional faces.

Methods—12 women with IPV-PTSD and 12 non-traumatized comparison women underwent BOLD functional magnetic resonance imaging while completing an emotional-face matching task.

Results—IPV-PTSD subjects relative to comparison subjects displayed increased activation of the anterior insula and amygdala and decreased connectivity among the anterior insula, amygdalae, and ACC while matching to fearful vs. happy target faces. A similar pattern of activation differences was also observed for angry vs. happy target faces. IPV-PTSD subjects relative to comparison subjects also displayed increased dACC/mPFC activation and decreased vACC activation when matching to a male vs. a female target, and the extent of increased dACC activation correlated positively with hyperarousal symptoms.

Conclusions—Women with IPV-PTSD display hyperactivity and disconnection among affective and limbic sensory systems while processing threat-related emotion. Furthermore, hyperactivity of cognitive-appraisal networks in IPV-PTSD may promote hypervigilant states of

Corresponding Author's Info: Greg Fonzo, 9500 Gilman Dr, MC 0855, La Jolla, CA 92093; gfonzo@ucsd.edu.

Financial Conflicts of Interest: The authors report no biomedical financial interests or potential conflicts of interest.

Publisher's Disclaimer: This is a PDF file of an unedited manuscript that has been accepted for publication. As a service to our customers we are providing this early version of the manuscript. The manuscript will undergo copyediting, typesetting, and review of the resulting proof before it is published in its final citable form. Please note that during the production process errors may be discovered which could affect the content, and all legal disclaimers that apply to the journal pertain.

awareness through an exaggerated sensitivity to contextual cues, i.e. male gender, which relate to past trauma.

Keywords

posttraumatic stress; anxiety; emotion; insula; amygdala; anterior cingulate

Introduction

Intimate-partner violence (IPV) is a worldwide public health problem (1), and a recent study identified IPV as the prime predictor of posttraumatic stress disorder (PTSD) among women (2). PTSD neuroimaging studies (Table S1 in Supplement 1) have produced evidence indicating abnormal function of two brain regions while processing threat-related emotional faces: the amygdala and the anterior cingulate/medial prefrontal cortex (ACC/mPFC). The amygdala processes the detection of salient perceptual stimuli and integration of secondary emotional responses, as demonstrated by its crucial role in the fear response and aversive conditioning (3,4). This neural structure is especially responsive to interpersonal signals of threat, such as fearful faces, and these stimuli have proven to be useful experimental probes of amygdala function in PTSD (5). The ACC/mPFC is involved in a diverse array of higher-order cognitive and affective functions (6). The ventral portion has been found to display hypoactive function in PTSD (7,8), often interpreted as evidence of emotional dysregulation (9). Currently, the amygdala and ACC/mPFC constitute the core PTSD neurocircuitry model of emotional dysfunction. However, the recent proposal of a neural system supporting interoception as well as evidence for the importance of interoceptive cues in the experience of emotion (10) suggests that a model of emotional dysfunction focused exclusively on the amygdala and ACC/mPFC may be incomplete.

Interoception is defined as the sense of the internal body state and includes a range of sensations such as pain, temperature, itch, tickle, and sensual touch. Taken together, these sensations provide an integrated sense of the body's physiological condition (11). The insular and anterior cingulate cortices have emerged as the primary neural substrates underlying interoceptive, i.e. limbic sensory processing and the subjective instantiation of feelings from the body, and they have also been demonstrated to be critically involved in processing emotion (12). Given the role of the insula in interoception and emotion as well as evidence indicating abnormal anterior insular function in anxious samples (13,14), this region has been proposed to serve a crucial role in proneness to anxiety through generation of an exaggerated interoceptive prediction signal, i.e. anticipated aversive body state (15). Although contemporary neurobiological models of anxiety focus on the amygdala, the proposal of abnormalities in insular function as contributing to pathological anxiety complements this prevailing theory by providing a neuroanatomical substrate capable of influencing the two primary components of anxiety—sympathetic hyperarousal and worry—through its diverse reciprocal connections to sites involved in affective and executive function (12). While the amygdala is critically involved in the fear response and states of sympathetic arousal, experimental evidence implicates the insula in more “diffuse” anxiety responses, such as anticipation (16) and avoidance (17).

While prior studies have focused on amygdala and ACC/mPFC dysfunction as underlying emotional dysregulation in PTSD, fewer studies have examined the role of potentially abnormal interoceptive cues. Therefore, we used a widely-published facial emotion processing task (18) which is associated with robust and reliable activation of insula and amygdala (19,20) to examine the neural substrates which are important for processing interoceptive cues. Specifically, we sought to test these neural substrates' response to threat-related emotion, e.g. by contrasting fearful relative to happy or neutral faces, which has

proven to be a useful comparison for eliciting limbic abnormalities in PTSD (21,22). There is some evidence that neutral faces may not be processed as “neutral” by anxious populations (23,24). Therefore, we chose happy faces as the comparator condition, which have also been used elsewhere with PTSD subjects to isolate threat-related emotion (9,27). Happy faces share similar interpersonal aspects with fearful faces but do not convey potential threat (25,26), which helps to delineate specific threat-related effects.

We also sought to examine two novel contrasts tailored to the IPV sample. Although all prior PTSD face-processing studies have used fearful faces to examine the limbic system, we hypothesized angry faces—another potential indicator of environmental threat (26)—might evoke limbic abnormalities due to the involvement of anger in the traumatic experience. Specifically, as perpetrators of IPV display more frequent and severe expressions of anger than non-violent men and are prone to respond to anger by becoming aggressive (28), we predicted angry faces might serve to elicit limbic hyperactivity in this sample due to the experiential association of this facial expression with subsequent environmental threat from an intimate partner. To test this hypothesis, we examined the contrast of processing angry relative to happy target faces as a secondary probe of emotional threat. As both angry and fearful faces activate the amygdala (29) and the insula (30) in normal populations, we expected contrasts for threat-related emotion to primarily evoke increased activation in these regions for the IPV-PTSD sample.

Second, individuals with PTSD show increased sensitivity to potential trauma cues (31). We suspected that faces of male gender might evoke a general state of hypervigilance in female IPV-PTSD subjects given the perpetration of trauma by a male intimate partner. It was hypothesized this hypervigilance would manifest as altered activation of “top-down” affective and cognitive-appraisal networks that are important for attention/arousal (32,33). Therefore, we examined the contrast of matching to a male relative to a female target face. While limbic hyperactivity in PTSD seems to reflect a “bottom-up” reactivity most readily evoked by threat-related emotional cues—consistent with amygdala (34) and insula (35) responsivity to nonconscious perception of fear—we expected a non-relevant, “contextual” stimulus characteristic such as face gender to primarily elicit changes in higher-order affective and cognitive regions involved in the coordination of emotion, attention, and arousal. Specifically, we expected that group differences related to face gender would primarily manifest as hypoactivation of the affective (ventral) subregion of the ACC/mPFC and hyperactivation of the cognitive (dorsal) subregion of ACC/mPFC, consistent with the emerging understanding of this pattern of ACC differences as potentially reflecting the deployment of attentional resources towards salient stimuli in the presence of activated arousal networks (36,37).

Methods

Subjects

Twelve non-treatment seeking women (n=12) exposed to IPV and 12 comparison subjects participated in BOLD functional magnetic resonance imaging (fMRI). IPV trauma was operationalized as physical and/or sexual abuse by a romantic partner occurring within five years of study recruitment and having ended by at least one month prior to recruitment (mean # of years of abuse=5.71, *s.d.*=7.10, range=.5-25.5). All women in the IPV-PTSD group met full DSM-IV criteria for PTSD due to IPV, verified through the Clinician-Administered PTSD Scale (CAPS; (38)) and the Structured Clinical Interview for Diagnosis-DSM IV (SCID-IV; (39)). Comparison subjects had never experienced a Criterion A traumatic event. Exclusionary criteria for both groups included: 1) substance abuse in the past year; 2) history of >2 years of alcohol abuse; 3) use of psychotropic medications in the past 4 weeks (or fluoxetine in the past 6 weeks); and 4) irremovable

ferromagnetic bodily material, pregnancy, claustrophobia, bipolar disorder, or schizophrenia. IPV-PTSD subjects with comorbid mood/anxiety disorders were included as long as PTSD was judged to be the clinically predominant disorder. Written informed consent was obtained from all subjects, and the study protocol was approved by the UCSD Human Research Protections Program and the VA San Diego Healthcare System Research and Development Office. Groups were matched on demographic variables except years of education, for which the IPV-PTSD group was significantly lower (see Table S2 in Supplement 1). Therefore, education was used as a covariate in all group comparisons.

Self-Report Psychological Measures

See Methods and Materials in Supplement 1 for a description of self-report measures.

Task

See Figure S1 in Supplement 1 for a depiction of the task.

Image Acquisition

Data were collected during task completion using fMRI image parameters sensitive to BOLD contrast on a 3.0T GE Signa EXCITE (GE Healthcare, Milwaukee, Wisconsin) scanner (T2*-weighted echo planar imaging, TR = 2000 msec, TE = 32 msec, field of view (FOV) = 250 × 250 mm, 64 × 64 matrix, 30 2.6mm axial slices with 1.4mm gap, 256 repetitions). A high-resolution T1-weighted image (172 sagittally acquired spoiled gradient recalled 1mm thick slices, inversion time (TI) = 450 msec, TR = 8 msec, TE = 4 msec, flip angle = 12 degrees, FOV = 250 × 250 mm) was also collected from each participant for anatomical reference. Images were preprocessed by interpolating voxel time-series data to correct for non-simultaneous slice acquisition in each volume.

Behavioral/Psychological Measure Data Analysis

Participant data for self-report and behavioral measures were subjected to a split-plot, repeated-measures ANOVA carried out in SPSS 15.0 (SPSS, Chicago, Illinois).

Image Processing/Analysis

Data were processed using the AFNI software package (40). Voxel time-series data was coregistered to an intra-run volume using a three-dimensional coregistration algorithm. Data was realigned to the anatomical space of each participant using AFNI's 3dAllineate. Voxel time-series data was corrected for artifact intensity spikes through fit to a smooth-curve function. Those time points with greater than 2 *s.d.* more voxel outliers than the subject's mean were excluded from analysis (as determined by the AFNI function 3dToutcount). As small motion corrections in translational and rotational dimensions are nearly collinear, only rotational parameters (roll, pitch, and yaw) were used as nuisance regressors for motion artifact. Two deconvolution analyses were conducted—one for emotional threat-related contrasts and one for the gender contrast. For emotional threat, the orthogonal regressors of interest were target trials of: 1) happy faces; 2) angry faces; 3) fearful faces; and 4) shapes. The outcome measures of interest were the linear contrasts of: 1) matching to a fearful vs. happy target; and 2) matching to an angry vs. happy target. For the gender contrast, the orthogonal regressors of interest were: 1) male target faces; 2) female target faces; and 3) shapes, for which the main outcome measure was the linear contrast of matching to a male vs. a female target; this contrast controls for emotion by averaging across this factor in each gender condition. Regressors of interest were convolved with a modified gamma-variate function to account for delay and dispersion of the hemodynamic response. Baseline and linear drift variables were also entered into the regression model. The average voxelwise response magnitude was fit and estimated using AFNI's 3dDeconvolve program. A Gaussian

smoothing filter with a full-width half max (FWHM) of 4 mm was applied to each participant's normalized voxelwise percent signal changes (PSCs) to account for individual variability in anatomical landmarks. Each subject's PSCs were normalized to Talairach coordinates using AFNI's built-in anatomical atlas (as specified by the Talairach Daemon) (41).

Whole-brain PSC data was entered into a one-sample voxel-based t-test to identify areas that activated significantly above the null for the effect of interest. An independent samples voxel-based t-test was used to identify areas significantly different between groups. A threshold adjustment based upon Monte-Carlo simulations (using AFNI's program AlphaSim) was used to guard against false positives in both the whole-brain and region-of-interest (ROI) analyses. *A-priori* voxelwise probability of $p < .05$ with a 4mm search radius and cluster size of 704 μl resulted in *a-posteriori* probability of $p < .05$. In addition to a whole-brain analysis, *a-priori* ROI analyses were conducted on brain regions implicated in emotion processing (bilateral insula, bilateral amygdala, and ventral/dorsal mPFC/ACC). Stereotactic coordinates of these ROIs were based on standardized locations taken from the Talairach atlas (42). Protection against Type-I error for voxelwise *a-priori* probability of $p < .05$ was obtained using cluster sizes of 192 μl for the amygdala, 320 μl for the insula, and 384 μl for the mPFC/ACC. Voxelwise activation values were extracted from areas of significant difference and subjected to further analysis in SPSS 15.0 for covariation of education.

Functional Connectivity Analyses

Functional connectivity analyses were conducted according to previously published methods (16). Data preprocessing involved correcting echoplanar signals for slice-dependent time shifts, Gaussian spatial smoothing with a 4.0mm FWHM kernel, and bandwidth filtering ($.009 < f < .08$). Normalization of images and censoring of outlier volumes was conducted as per activation analyses. In keeping with the experimental design of prior PTSD investigations of connectivity during emotion processing (21,22), individual timecourses were extracted from each participant's preprocessed echoplanar time-series for seed ROIs in the amygdala, ACC, and anterior insula showing task-dependent ROI activation for the fearful vs. happy target contrast. The psychophysiological interaction (PPI) of the time-course for each seed ROI and the effects-coded contrast of fearful vs. happy targets was calculated and entered into the deconvolution as the outcome variable of interest, along with task, movement, baseline, and linear drift regressors. An independent-sample t-test was used to examine group differences in voxelwise Fisher-Z transformed correlation coefficients for the PPI. This connectivity difference map was then masked for ROI analysis in *a-priori* regions of interest using the same technique (see above) to guard against false-positives. Voxelwise correlation coefficients were extracted from clusters of significant difference and were entered into SPSS 15.0 for covariation of education.

Brain Activation Relationships with Self-Report Psychological Measures

Relationships between imaging data and written measures were assessed using voxelwise univariate regressions. IPV-PTSD participant subscales/total scores were regressed on individual activation maps. These scale-activation regression maps were masked for *a-priori* ROIs, thresholded at $p < .05$, and clustered for minimum significant volume according to Monte-Carlo simulations (as above). To identify IPV-PTSD functional differences associated with symptoms, these scale-activation regression maps were conjoined with the Type-I error-protected between-group ROI activation map and examined for significant overlap (as determined by Monte-Carlo simulations on group effect clusters). Voxelwise activation values for areas of significant overlap were extracted and entered into SPSS 15.0 for confirmation of significance using Spearman's ρ , a nonparametric correlation which is

robust to outliers. It should be noted that we did not restrict our experiment-wise α level to .05 across all self-report measures when performing correlational analyses. As we used a conservative method for examining brain-behavior relationships which did not employ circular analyses—which can decrease voxelwise variability and inflate the magnitude of a correlation (43,44)—we felt that retaining a voxelwise α level of .05 for each self-report measure scale would strike the most judicious balance between maximizing power and minimizing false-positives.

Results

Emotional Face Matching Task Behavioral Data

There were no performance differences between IPV-PTSD subjects and comparison subjects as measured by response latency (repeated-measures ANOVA covaried for education— $F_{Group}(1,20)=.771$, $p=.39$; $F_{Group \times Emotion}(2,19)=.952$, $p=.625$; $F_{Group \times Gender}(1,20)=.947$, $p=.304$; $F_{Group \times Emotion \times Gender}(2,19)=.853$, $p=.222$) or accuracy ($F_{Group}(1,20)=3.672$, $p=.07$; $F_{Group \times Emotion}(2,19)=.892$, $p=.339$; $F_{Group \times Gender}(1,20)=.938$, $p=.263$; $F_{Group \times Emotion \times Gender}(2,19)=.844$, $p=.199$; See Table S3 in Supplement 1).

Brain Activation

See Tables S4 – S7 in Supplement 1 for results of task effect activation and connectivity analyses. All group differences reported below remained significant after covarying for education, and statistics are reported with education covaried out.

Threat-Related Emotion Contrast (1): Fearful Relative to Happy Target Faces

—Between-group comparisons in *a-priori* ROIs revealed significantly increased activation for the IPV-PTSD group in the left anterior insula and the right amygdala (Figure 1); whole-brain analysis also identified increased activation in brainstem, left middle frontal gyrus (MFG), and left precentral gyrus and decreased activation in the right middle temporal gyrus (MTG; Table 1).

Threat-Related Emotion Contrast (2): Angry Relative to Happy Target Faces—

Between-group comparisons in *a-priori* ROIs revealed significantly increased activation for the IPV-PTSD group in the right mid-insula, the left anterior insula, and the right amygdala (Table 2 and Figure 1). Whole-brain analyses also showed these insular differences while revealing increased activation in areas such as the left precuneus, left cingulate gyrus, left MTG and superior temporal gyrus, as well as decreased activation in the right MFG.

Gender Contrast: Male Relative to Female Target Faces—

Between-group comparisons in *a-priori* ROIs revealed significantly greater activation for the IPV-PTSD group in the bilateral dACC and significantly reduced activation in the ventral and subgenual ACC (vsgACC; Table 3 and Figure 2). Whole-brain analyses also showed these differences while demonstrating increased activation in the bilateral dorsomedial frontal gyri, left MTG, right supramarginal gyrus, right precuneus, and left precentral gyrus.

Activation Brain/Behavior Relationships

The conjunction of the group \times task effect map and the PCL-C and IES-R univariate regression maps in the IPV-PTSD group for matching to male relative to female faces revealed hyperactivation in the dACC/medial frontal gyri which was positively correlated with hyperarousal (PCL-C Hyperarousal subscale: mean $\rho=.695$, mean $p=.029$; IES-R Hyperarousal subscale: mean $\rho=.586$, mean $p=.017$; Figure S2 in Supplement 1). That is, greater hyperactivation in this region was associated with greater symptoms of hyperarousal. There were no significant regions of correlated activity identified with conjunctions of

threat-related emotion contrasts or with conjunctions of remaining subscales of the PCL-C, IES-R, CTQ, CTS-2, or BDI; that is, there was no relationship between childhood trauma, past IPV trauma history/severity/type, or depression and patterns of group differences.

Functional Connectivity for Matching to a Fearful Relative to Happy Target Face

Between-group ROI analyses (Figure 3; Table 4) revealed significantly smaller correlation coefficients in the IPV-PTSD group in the left anterior insula with activity in a dACC seed ROI. Second, voxels in the left amygdala for the IPV-PTSD group were significantly less correlated with activity in the left anterior insula seed ROI. Third, the left anterior insula, left mid-insula, right mid-insula, and bilateral amygdalae showed significantly weaker correlations in the IPV-PTSD group with activity in a second, more dorsal left anterior insula seed ROI. Fourth, voxels in the left anterior insula in the IPV-PTSD group were more weakly correlated with activity in the right amygdala seed ROI. Significantly stronger correlations with activity in the dACC seed ROI for the IPV-PTSD group were observed in the right posterior insula, and IPV-PTSD sgACC activity was more strongly correlated with that in the right amygdala seed ROI.

Discussion

This investigation yielded three main findings. First, the anterior insula and amygdala of IPV-PTSD subjects was more active when individuals processed fearful or angry target faces. Second, at the same time this increased activation occurred with attenuated connectivity among the dACC, anterior insula, and amygdalae during the processing of fearful faces. Third, the dACC/mPFC of IPV-PTSD subjects was more active when matching to a male vs. a female target face, which was positively correlated with hyperarousal symptoms. Taken together, the limbic system activation pattern in IPV-PTSD individuals is consistent with exaggerated and functionally disconnected processing of threat-related affective stimuli. Moreover increased activation of “top-down” cognitive-appraisal neural structures such as the dACC may contribute to arousal dysregulation through promoting hypervigilance and/or an attentional bias towards contextual cues which relate to prior trauma.

These results demonstrate that PTSD is characterized by hyperactivity of both the amygdala and anterior insula during the processing of threat-related emotion. Furthermore, the replication of amygdalar hyperactivity within an expanded face-processing paradigm reflects favorably on the external validity of the findings of prior PTSD imaging studies (Figure 1). Fearful faces were originally utilized as nonspecific signals of threat to demonstrate the pervasive nature of PTSD limbic dysregulation (27). To our knowledge, this study presents the first evidence that angry faces may also serve as nonspecific signals of threat which are capable of eliciting limbic hyperactivity in IPV-PTSD subjects. It is possible that both fearful and angry faces signal the need to engage in self-preservative actions. Thus, increased activation of “bottom-up” limbic structures implicated in the detection of salient stimuli and representation of internal body states (29,30) in PTSD individuals may indicate an overgeneralization of exaggerated responding to certain emotional cues other than fear, *per se*. However, given the involvement of anger in IPV trauma, studies in other trauma samples are needed to determine if this limbic hyperactivity reflects a more “general” threat-related functional abnormality or is more specific to the experience of IPV trauma.

We observed decreased vACC and increased dACC activation for matching to a male vs. a female face, partially consistent with results of prior PTSD face-processing studies (9). While vACC hypoactivity has been interpreted to reflect emotional dysregulation (45), other studies have identified a hyperactive dorsal ACC/mPFC network in PTSD which may be involved in “hypervigilant” attention and arousal (33,46). To our knowledge, this is the first

PTSD face-processing study which has dissociated amygdalar and ACC/mPFC abnormalities to the same emotional faces using contrasts which respectively capture emotional threat and face gender, consistent with recent findings suggesting ACC abnormalities in PTSD extend to the processing of salient non-emotional stimuli (36,37). Given the role of ACC in modulating arousal (47) and attention/vigilance (48) and in appraising self-relevance of stimuli (49), these results suggest hyperactivity of the dACC while matching to a male face reflects a general state of hypervigilance potentially secondary to an attentional bias for “contextual” stimulus characteristics related to past trauma. This interpretation is consistent with the proposal of the dACC as an intermediary between emotion and attention (33), evidence for an attentional bias in PTSD towards trauma-related information (50), as well as the hypothesis that dysregulated appraisal, representation, and integration of contextual cues underlies ACC/mPFC abnormalities in PTSD (51). In conjunction with the correlation of dACC hyperactivity with hyperarousal, these results suggest this hypervigilance/attentional bias may exacerbate arousal dysregulation through repeated overengagement of cognitive resources subserving action-readiness in response to trauma-related contextual cues. It should be noted that we lack corroborating data (e.g., anxiety ratings) to support the contention that male faces were experienced differently by the IPV-PTSD group. This remains to be explored in future studies, and the differences in brain function observed here can only speculatively be attributed to degree of trauma-relevance. It should also be underscored that this dACC-hyperarousal correlation is in need of replication in extended PTSD samples.

This study has several limitations. First, although we interpreted each emotion condition according to that of the target face, it should be noted that these trials do not represent “pure” depictions of the emotion in question due to the presence of an emotional distractor; therefore, these threat-related contrasts are not directly comparable with those of prior PTSD studies. Second, the IPV-PTSD group consisted only of women with exposure to IPV, so these findings may not be generalizable to males or to other forms of PTSD. Third, as we did not have access to a trauma-exposed comparison group who never developed PTSD after IPV exposure, we cannot tell if these results are due to the experience of IPV, the development of PTSD, or both. Fourth, we chose to include IPV-PTSD participants with comorbid depression or other anxiety disorders, which may represent a threat to internal validity. However, given the frequent comorbidity seen in IPV-PTSD, we felt it most appropriate to recruit a sample generalizable to women with IPV-PTSD in the population and use secondary correlational analyses to examine how different symptom dimensions might be contributing to findings. Although our analyses suggest comorbid disorders are not contributing to results, power to test for such effects is low, and future studies are needed to dissociate if/how comorbid disorders may be contributing to patterns of group differences. Fifth, our sample size was relatively modest for a PTSD imaging study, and power to detect group differences was limited. Sixth, our use of happy faces as the comparator condition raises the possibility that differences in brain function to accepting as well as threatening stimuli may be contributing to group differences (i.e., IPV-PTSD women may show blunted insular/amygdalar responses to happy faces). Seventh, as angry male faces might be expected to elicit the greatest group differences in this sample, we were unable to examine the potential interaction effect of emotion x gender of target face due to power constraints. Lastly, our IPV-PTSD sample was significantly less educated than the control sample; although the findings were largely unchanged by the inclusion of education as a covariate, the results could reflect subtle differences in pre-trauma intellectual ability, thought to be a risk-factor for development of PTSD (52,53).

Supplementary Material

Refer to Web version on PubMed Central for supplementary material.

Acknowledgments

This work was supported by research grant MH64122 from the National Institute of Mental Health and a VA Merit Grant, both to MBS. SRT would like to thank Tara Short, B.A. for her contribution to the project. SBN would like to thank Karla Espinosa de los Monteros, M.S. for her contribution to the project.

References

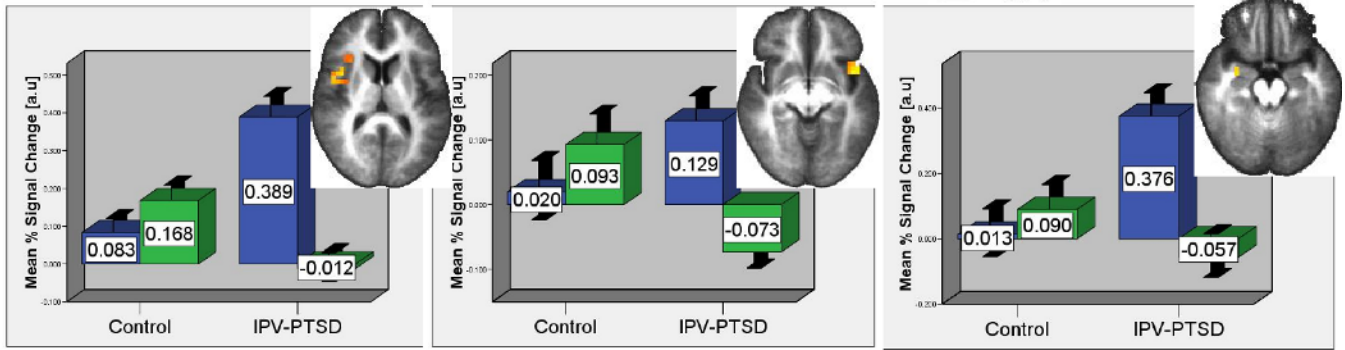
1. Dejonghe ES, Bogat GA, Levendosky AA, Eye A. Women survivors of intimate partner violence and post-traumatic stress disorder: Prediction and prevention. *J Postgrad Med* 2008;54:294–300. [PubMed: 18953149]
2. Pico-Alfonso MA. Psychological intimate partner violence: the major predictor of posttraumatic stress disorder in abused women. *Neurosci Biobehav Rev* 2005;29:181–193. [PubMed: 15652265]
3. Costafreda SG, Brammer MJ, David AS, Fu CH. Predictors of amygdala activation during the processing of emotional stimuli: a meta-analysis of 385 PET and fMRI studies. *Brain Res Rev* 2008;58:57–70. [PubMed: 18076995]
4. Sergerie K, Chochol C, Armony JL. The role of the amygdala in emotional processing: a quantitative meta-analysis of functional neuroimaging studies. *Neurosci Biobehav Rev* 2008;32:811–830. [PubMed: 18316124]
5. Liberzon I, Sripada CS. The functional neuroanatomy of PTSD: a critical review. *Prog Brain Res* 2008;167:151–169. [PubMed: 18037013]
6. Amodio DM, Frith CD. Meeting of minds: the medial frontal cortex and social cognition. *Nat Rev Neurosci* 2006;7:268–277. [PubMed: 16552413]
7. Kim MJ, Chey J, Chung A, Bae S, Khang H, Ham B, et al. Diminished rostral anterior cingulate activity in response to threat-related events in posttraumatic stress disorder. *J Psychiatr Res* 2008;42:268–277. [PubMed: 17400251]
8. Shin LM, Rauch SL, Pitman RK. Amygdala, medial prefrontal cortex, and hippocampal function in PTSD. *Ann N Y Acad Sci* 2006;1071:67–79. [PubMed: 16891563]
9. Shin LM, Wright CI, Cannistraro PA, Wedig MM, McMullin K, Martis B, et al. A functional magnetic resonance imaging study of amygdala and medial prefrontal cortex responses to overtly presented fearful faces in posttraumatic stress disorder. *Arch Gen Psychiatry* 2005;62:273–281. [PubMed: 15753240]
10. Craig AD. Human feelings: Why are some more aware than others? *Trends Cogn Sci (Regul Ed)* 2004;8:239–241. [PubMed: 15165543]
11. Craig AD. Interoception: the sense of the physiological condition of the body. *Curr Opin Neurobiol* 2003;13:500–505. [PubMed: 12965300]
12. Craig AD. How do you feel--now? The anterior insula and human awareness. *Nat Rev Neurosci* 2009;10:59–70. [PubMed: 19096369]
13. Stein MB, Simmons AN, Feinstein JS, Paulus MP. Increased amygdala and insula activation during emotion processing in anxiety-prone subjects. *Am J Psychiatry* 2007;164:318–327. [PubMed: 17267796]
14. Etkin A, Wager TD. Functional neuroimaging of anxiety: a meta-analysis of emotional processing in PTSD, social anxiety disorder, and specific phobia. *Am J Psychiatry* 2007;164:1476–1488. [PubMed: 17898336]
15. Paulus MP, Stein MB. An insular view of anxiety. *Biol Psychiatry* 2006;60:383–387. [PubMed: 16780813]
16. Simmons AN, Paulus MP, Thorp SR, Matthews SC, Norman SB, Stein MB. Functional activation and neural networks in women with posttraumatic stress disorder related to intimate partner violence. *Biol Psychiatry* 2008;64:681–690. [PubMed: 18639236]
17. Samanez-Larkin GR, Hollon NG, Carstensen LL, Knutson B. Individual differences in insular sensitivity during loss: Anticipation predict avoidance learning. *Psychological Science* 2008;19:320–323. [PubMed: 18399882]

18. Hariri AR, Drabant EM, Munoz KE, Kolachana BS, Mattay VS, Egan MF, et al. A Susceptibility Gene for Affective Disorders and the Response of the Human Amygdala. *Arch Gen Psychiatry* 2005;62:146–152. [PubMed: 15699291]
19. Stein MB, Simmons AN, Feinstein JS, Paulus MP. Increased amygdala and insula activation during emotion processing in anxiety-prone subjects. *Am J Psychiatry* 2007;164:318–327. [PubMed: 17267796]
20. Paulus MP, Feinstein JS, Castillo G, Simmons AN, Stein MB. Dose-Dependent Decrease of Activation in Bilateral Amygdala and Insula by Lorazepam During Emotion Processing. *Arch Gen Psychiatry* 2005;62:282–288. [PubMed: 15753241]
21. Bryant RA, Kemp AH, Felmingham KL, Liddell B, Olivieri G, Peduto A, et al. Enhanced amygdala and medial prefrontal activation during nonconscious processing of fear in posttraumatic stress disorder: an fMRI study. *Hum Brain Mapp* 2008;29:517–523. [PubMed: 17525984]
22. Williams LM, Kemp AH, Felmingham K, Barton M, Olivieri G, Peduto A, et al. Trauma modulates amygdala and medial prefrontal responses to consciously attended fear. *Neuroimage* 2006;29:347–357. [PubMed: 16216534]
23. Cooney RE, Atlas LY, Joormann J, Eugene F, Gotlib IH. Amygdala activation in the processing of neutral faces in social anxiety disorder: is neutral really neutral? *Psychiatry Res* 2006;148:55–59. [PubMed: 17030117]
24. Arce E, Simmons AN, Stein MB, Winkielman P, Hitchcock C, Paulus MP. Association between individual differences in self-reported emotional resilience and the affective perception of neutral faces. *J Affect Disord* 2009;114:286–293. [PubMed: 18957273]
25. Mehu M, Little AC, Dunbar RIM. Sex differences in the effect of smiling on social judgments: An evolutionary approach. *Journal of Social, Evolutionary, and Cultural Psychology* 2008;2:103–121.
26. Dimberg U, Öhman A. Behold the wrath: Psychophysiological responses to facial stimuli. Motivation and Emotion. Special Issue: Facial Expression and Emotion—The Legacy of John T Lanzetta, Part I 1996;20:149–182.
27. Rauch SL, Whalen PJ, Shin LM, McInerney SC, Macklin ML, Lasko NB, et al. Exaggerated amygdala response to masked facial stimuli in posttraumatic stress disorder: a functional MRI study. *Biol Psychiatry* 2000;47:769–776. [PubMed: 10812035]
28. Eckhardt CI, Samper RE, Murphy CM. Anger disturbances among perpetrators of intimate partner violence: Clinical characteristics and outcomes of court-mandated treatment. *J Interpers Violence* 2008;23:1600–1617. [PubMed: 18378815]
29. Derntl B, Habel U, Windischberger C, Robinson S, Kryspin-Exner I, Gur RC, et al. General and specific responsiveness of the amygdala during explicit emotion recognition in females and males. *BMC Neuroscience* 2009;10
30. Grosbras M, Paus T. Brain Networks Involved in Viewing Angry Hands or Faces. *Cerebral Cortex* 2006;16:1087–1096. [PubMed: 16221928]
31. Litz BT, Orsillo SM, Kaloupek D, Weathers F. Emotional processing in posttraumatic stress disorder. *J Abnorm Psychol* 2000;109:26–39. [PubMed: 10740933]
32. Morey RA, Dolcos F, Petty CM, Cooper DA, Hayes JP, Labar KS, et al. The role of trauma-related distractors on neural systems for working memory and emotion processing in posttraumatic stress disorder. *J Psychiatr Res*. 2008
33. Pannu Hayes J, Labar KS, Petty CM, McCarthy G, Morey RA. Alterations in the neural circuitry for emotion and attention associated with posttraumatic stress symptomatology. *Psychiatry Res* 2009;172:7–15. [PubMed: 19237269]
34. Kemp AH, Felmingham KL, Falconer E, Liddell BJ, Bryant RA, Williams LM. Heterogeneity of non-conscious fear perception in posttraumatic stress disorder as a function of physiological arousal: an fMRI study. *Psychiatry Res* 2009;174:158–161. [PubMed: 19836929]
35. Felmingham K, Kemp AH, Williams L, Falconer E, Olivieri G, Peduto A, et al. Dissociative responses to conscious and non-conscious fear impact underlying brain function in post-traumatic stress disorder. *Psychol Med* 2008;38:1771–1780. [PubMed: 18294420]
36. Felmingham KL, Williams LM, Kemp AH, Rennie C, Gordon E, Bryant RA. Anterior cingulate activity to salient stimuli is modulated by autonomic arousal in Posttraumatic Stress Disorder. *Psychiatry Res* 2009;173:59–62. [PubMed: 19446442]

37. Bryant RA, Felmingham KL, Kemp AH, Barton M, Peduto AS, Rennie C, et al. Neural networks of information processing in posttraumatic stress disorder: a functional magnetic resonance imaging study. *Biol Psychiatry* 2005;58:111–118. [PubMed: 16038681]
38. Blake DD, Weathers FW, Nagy LM, Kaloupek DG. The development of a Clinician-Administered PTSD Scale. *J Trauma Stress* 1995;8:75–90. [PubMed: 7712061]
39. First, MB.; Spitzer, RL.; Gibbon, M.; Williams, JBW. Structured Clinical Interview for DSM-IV Axis I Disorders. New York: Biometrics Research, New York State Psychiatric Institute; 1998.
40. Cox RW. AFNI: software for analysis and visualization of functional magnetic resonance neuroimages. *Comput Biomed Res* 1996;29:162–173. [PubMed: 8812068]
41. Lancaster JL, Woldorff MG, Parsons LM, Liotti M, Freitas CS, Rainey L, et al. Automated Talairach atlas labels for functional brain mapping. *Hum Brain Mapp* 2000;10:120–131. [PubMed: 10912591]
42. Talairach, J.; Tournoux, P. Co-planar Stereotaxic Atlas of the Human Brain: 3-Dimensional Proportional System: An Approach to Cerebral Imaging. New York: Thieme Medical Publishers; 1998.
43. Kriegeskorte N, Simmons WK, Bellgowan PS, Baker CI. Circular analysis in systems neuroscience: the dangers of double dipping. *Nat Neurosci* 2009;12:535–540. [PubMed: 19396166]
44. Vul E, Harris C, Winkielman P, Pashler H. Puzzlingly high correlations in fMRI studies of emotion, personality, and social cognition. *Perspectives on Psychological Science* 2009;4:274–290.
45. Rauch SL, Shin LM, Phelps EA. Neurocircuitry models of posttraumatic stress disorder and extinction: human neuroimaging research—past, present, and future. *Biol Psychiatry* 2006;60:376–382. [PubMed: 16919525]
46. Morey RA, Dolcos F, Petty CM, Cooper DA, Hayes JP, Labar KS, et al. The role of trauma-related distractors on neural systems for working memory and emotion processing in posttraumatic stress disorder. *J Psychiatr Res*. 2008
47. Critchley HD, Mathias CJ, Josephs O, O'Doherty J, Zanini S, Dewar BK, et al. Human cingulate cortex and autonomic control: converging neuroimaging and clinical evidence. *Brain* 2003;126:2139–2152. [PubMed: 12821513]
48. Clark VP, Fannon S, Lai S, Benson R, Bauer L. Responses to rare visual target and distractor stimuli using event-related fMRI. *J Neurophysiol* 2000;83:3133–3139. [PubMed: 10805707]
49. Phan KL, Taylor SF, Welsh RC, Ho SH, Britton JC, Liberzon I. Neural correlates of individual ratings of emotional salience: a trial-related fMRI study. *Neuroimage* 2004;21:768–780. [PubMed: 14980580]
50. Amir N, Coles ME, Foa EB. Automatic and strategic activation and inhibition of threat-relevant information in posttraumatic stress disorder. *Cognitive Therapy and Research* 2002;26:645–655.
51. Liberzon, I.; Garfinkel, SN. Functional neuroimaging in post-traumatic stress disorder. In: Shiromani, Priyattam J.; Keane, Terence M.; LeDoux, Joseph E., editors. Post-traumatic stress disorder: Basic science and clinical practice. Totowa, NJ, US: Humana Press; 2009. p. 297-317.
52. Gurvits TV, Metzger LJ, Lasko NB, Cannistraro PA, Tarhan AS, Gilbertson MW, et al. Subtle neurologic compromise as a vulnerability factor for combat-related posttraumatic stress disorder: results of a twin study. *Arch Gen Psychiatry* 2006;63:571–576. [PubMed: 16651514]
53. Kremen WS, Koenen KC, Boake C, Purcell S, Eisen SA, Franz CE, et al. Pretrauma cognitive ability and risk for posttraumatic stress disorder: a twin study. *Arch Gen Psychiatry* 2007;64:361–368. [PubMed: 17339525]

Angry Target vs. Happy Target

Angry
Happy



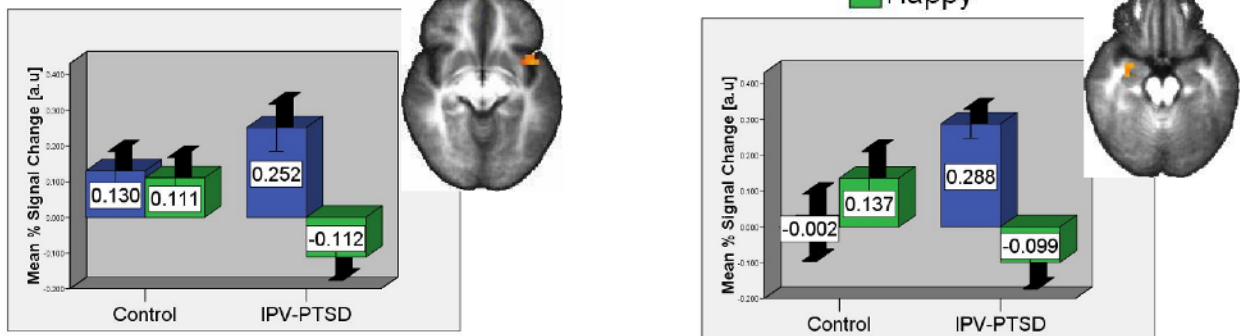
Right Middle Insula

Left Anterior Insula

Right Amygdala

Fearful Target vs. Happy Target

Fear
Happy



Left Anterior Insula

Right Amygdala

Figure 1.

Increased Insular & Amygdalar Activation for IPV-PTSD vs. Controls for Matching to a Fearful or Angry vs. Happy Target Face

Graphs depict average voxelwise % signal changes for trials of each emotional expression vs. the sensorimotor baseline. Error bars depict +/- 1 standard error.

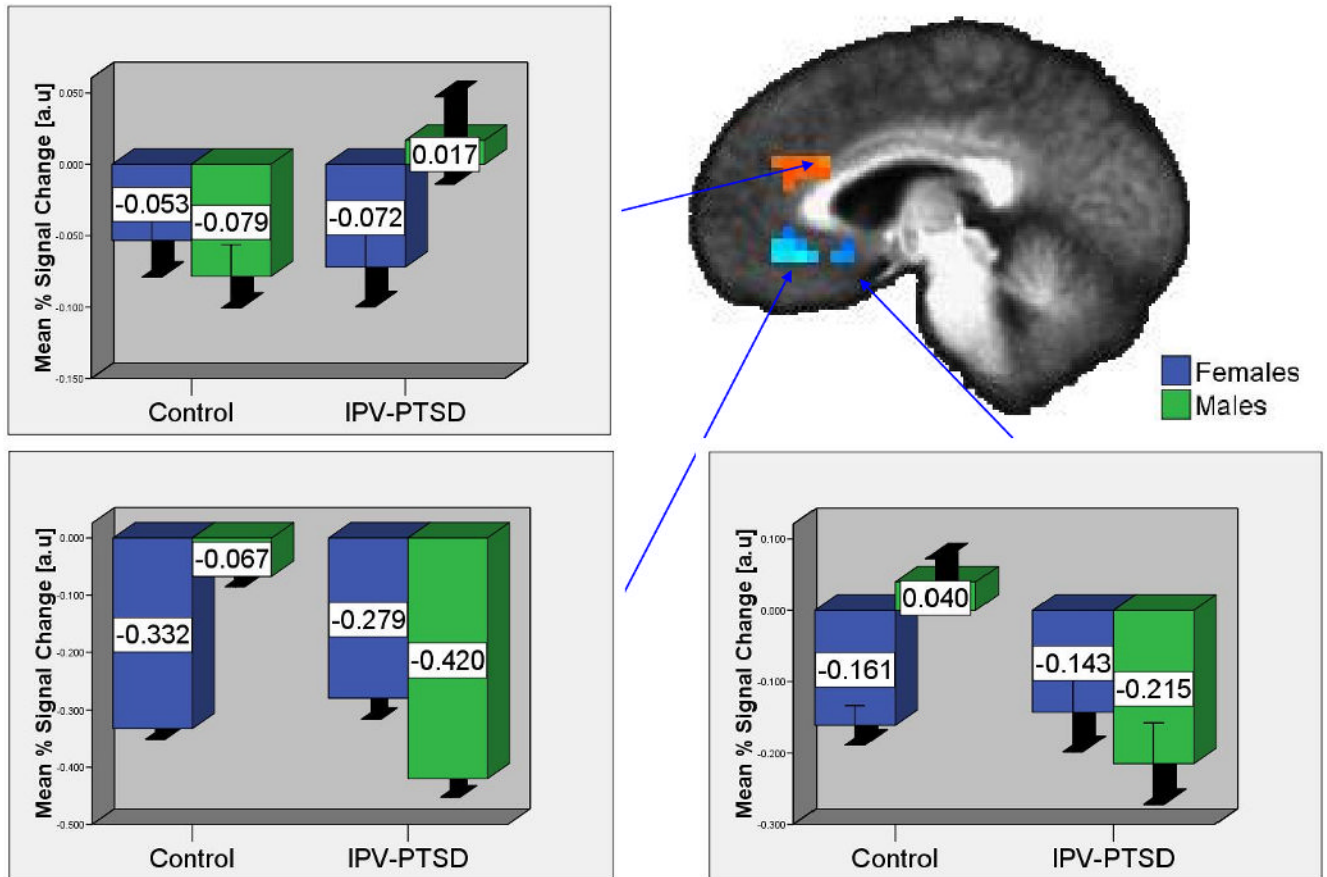


Figure 2.
Anterior Cingulate Activation Differences for IPV-PTSD vs. Controls for Matching to a Male vs. Female Target Face
Graphs depict average voxelwise % signal changes for faces of each gender vs. the sensorimotor baseline. Error bars depict +/- 1 standard error.

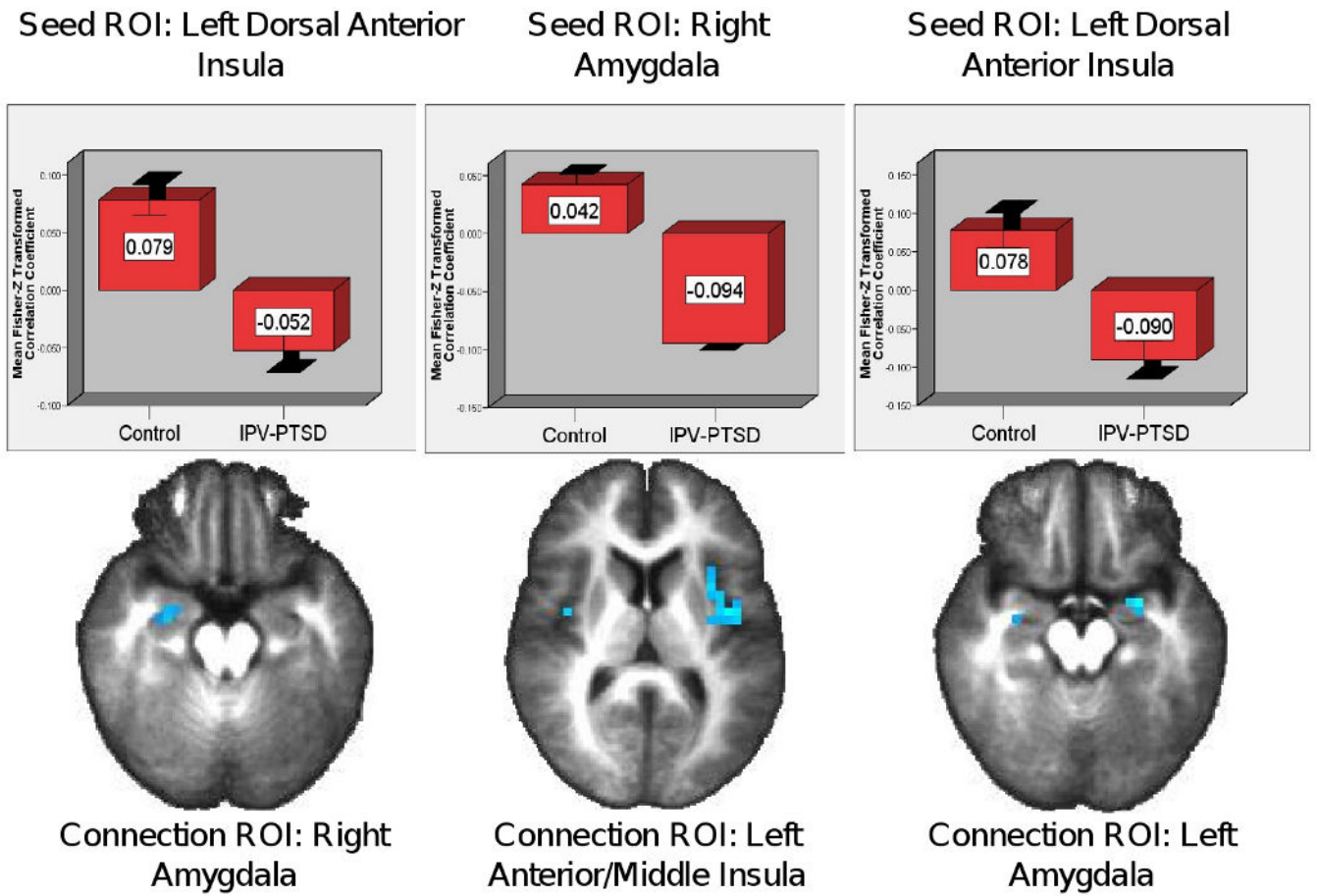


Figure 3. Significantly Reduced Insular-Amygdalar Connectivity for IPV-PTSD vs. Controls for Matching to a Fearful vs. Happy Target Face
 Graphs depict average voxelwise Fisher-Z transformed correlation coefficients. Error bars depict ± 2 standard deviations.

Table 1

Areas of Significantly Increased or Decreased Activation for IPV-PTSD vs. Controls for Matching to a Fearful vs. Happy Target Face

| Analysis | Side | Anatomical Area | Size (μ l) | X | Y | Z | Voxelwise Statistics: Mean (SD) | |
|----------|------|---------------------------|-----------------|-------|-------|-------|---------------------------------|-------------|
| | | | | | | | F* | P* |
| ROI | L | Insula (a) | 448 | -41.4 | 8.0 | -4.6 | 6.035 (1.68) | .028 (.016) |
| ROI | R | Amygdala | 320 | 28.4 | -3.4 | -15.3 | 5.277 (0.50) | .032 (.007) |
| WB | B | Brainstem | 2304 | -3.5 | -34.4 | -36.2 | 7.439 (3.81) | .025 (.018) |
| WB | L | Middle Frontal Gyrus | 896 | -44.7 | 16.9 | 29.9 | 7.250 (2.87) | .023 (.019) |
| WB | L | Precentral Gyrus | 896 | -44.2 | -7.1 | 37.9 | 6.698 (2.34) | .024 (.017) |
| WB | R | Middle Temporal Gyrus (-) | 832 | 45.7 | -71.0 | 14.2 | 8.307 (4.03) | .016 (.012) |

Cluster coordinates and anatomical areas are for cluster center of mass as defined by Talairach stereotactic space; Negative (-) signs following anatomical area indicate reduced activation; Descriptors for insula clusters do not reflect stereotactic distinctions, but are estimates based upon the relative location of activation on the group map

* Voxelwise statistics are presented with education covaried out; ROI=region of interest; WB=whole brain; a=anterior insula.

Table 2

Areas of Significantly Increased or Decreased Activation for IPV-PTSD vs. Controls for Matching to an Angry vs. Happy Target Face

| Analysis | Side | Anatomical Area | Size (μ l) | X | Y | Z | Voxelwise Statistics: Mean (SD) | |
|----------|------|--------------------------------|-----------------|-------|-------|------|---------------------------------|-------------|
| | | | | | | | F* | p* |
| ROI | R | Insula (m) | 704 | 41.2 | 4.5 | 12.8 | 6.410 (2.60) | .027 (.016) |
| ROI | L | Insula (a) | 512 | -42.1 | 10 | -4 | 5.931 (1.49) | .029 (.017) |
| ROI | R | Amygdala | 256 | 30 | -4.5 | 14.5 | 5.702 (1.30) | .029 (.014) |
| WB | L | Precuneus | 1344 | -11.3 | -51.4 | 43.6 | 8.234 (3.62) | .018 (.015) |
| WB | L | Cingulate Gyrus | 1088 | -5.4 | 2.5 | 32.1 | 4.847 (0.55) | .040 (.010) |
| WB | L | Middle Temporal Gyrus | 896 | -56.1 | -6.0 | -7.7 | 5.663 (1.83) | .035 (.023) |
| WB | R | Insula (m) | 832 | 42.6 | 4.0 | 12.7 | 5.717 (2.48) | .038 (.027) |
| WB | L | Precentral Gyrus | 832 | -32.9 | -9.7 | 34.1 | 8.648 (3.74) | .017 (.012) |
| WB | L | Superior Temporal Gyrus/Insula | 768 | -45.2 | 10.6 | -4.3 | 6.569 (1.63) | .023 (.017) |
| WB | L | Precentral Gyrus | 768 | -25.1 | -22.3 | 44.7 | 6.801 (2.22) | .023 (.017) |
| WB | L | Cerebellar Tonsil | 704 | -35.5 | -40.8 | -31 | 4.895 (0.57) | .039 (.010) |
| WB | R | Middle Frontal Gyrus (-) | 704 | 29.1 | 59.0 | 12.3 | 7.891 (3.29) | .016 (.009) |

Cluster coordinates and anatomical areas are for cluster center of mass as defined by Talairach stereotactic space; Negative (-) signs following anatomical area indicate reduced activation; Descriptors for insula clusters do not reflect stereotactic distinctions, but are estimates based upon the relative location of activation on the group map;

* Voxelwise statistics are presented with education covaried out; ROI=region of interest; WB=whole brain; m=middle insula; a=anterior insula.

Table 3

Areas of Significantly Increased or Decreased Activation for IPV-PTSD vs. Controls for Matching to a Male vs. Female Target Face

| Analysis | Side | Anatomical Area | Size (nl) | X | Y | Z | Voxelwise Statistics: Mean (SD) | |
|----------|------|--------------------------------|-----------|-------|-------|------|---------------------------------|-------------|
| | | | | | | | F* | P* |
| ROI | B | Ventral ACC (-) | 1664 | 0.1 | 35.1 | -5.6 | 6.310 (2.14) | .028 (.020) |
| ROI | B | Dorsal ACC | 1088 | 1.6 | 31.4 | 22.2 | 9.091 (3.70) | .014 (.015) |
| ROI | L | Subgenual ACC (-) | 576 | -4.4 | 16.9 | -8.3 | 4.640 (1.18) | .048 (.010) |
| WB | B | Dorsal ACC/Medial Frontal Gyri | 4992 | 3.5 | 43.7 | 22.7 | 8.350 (4.26) | .020 (.028) |
| WB | L | Middle Temporal Gyrus | 2432 | -43.6 | -60.7 | 19.7 | 6.192 (1.86) | .030 (.025) |
| WB | B | Ventral ACC (-) | 1664 | 0.1 | 35.1 | -5.6 | 6.443 (2.09) | .026 (.016) |
| WB | R | Supramarginal Gyrus | 1536 | 39.9 | -49.3 | 34.1 | 9.080 (2.67) | .010 (.008) |
| WB | R | Precuneus | 960 | 17.4 | -62.6 | 34.2 | 7.255 (2.58) | .022 (.019) |
| WB | L | Precentral Gyrus | 896 | -48.1 | -8.6 | 32.4 | 5.495 (1.59) | .037 (.028) |

Cluster coordinates and anatomical areas are for cluster center of mass as defined by Talairach stereotactic space; Negative (-) signs following anatomical area indicate a relative deactivation; Descriptors for ACC clusters do not reflect stereotactic distinctions, but are estimates based upon the relative location of activation on the group map;

* Voxelwise statistics are presented with education covaried out; ROI=region of interest; WB=whole brain.

Table 4
Significant Connectivity Differences for IPV-PTSD vs. Controls for Matching to a Fearful vs. Happy Target Face

| Seed ROI | Side | Connection ROI | Size(μ l) | X | Y | Z | Voxelwise Statistics: Mean (S.D.) | |
|-----------------|------|-----------------|----------------|-------|-------|-------|-----------------------------------|-------------|
| | | | | | | | F* | p* |
| Dorsal ACC | R | Insula (p) | 384 | 38 | -28.3 | 17.4 | 6.250 (1.94) | .016 (.006) |
| | L | Insula (a)(-) | 320 | -41.9 | 11 | 12 | 9.064 (1.74) | .008 (.005) |
| Left Insula (a) | L | Amygdala (-) | 448 | -18.6 | -5 | -16.5 | 6.760 (3.07) | .035 (.017) |
| | L | Insula (a)(-) | 448 | -42.3 | 9.9 | 12.6 | 10.256 (3.06) | .007 (.005) |
| Left Insula (a) | L | Insula (a)(-) | 640 | -35.5 | 13.9 | -5.8 | 11.233 (5.21) | .013 (.022) |
| | L | Insula (a/m)(-) | 640 | -41.8 | 10.1 | 11.2 | 5.992 (2.03) | .035 (.027) |
| | R | Insula (p)(-) | 512 | 41.4 | -12.4 | 4.9 | 7.017 (3.03) | .025 (.020) |
| | R | Amygdala (-) | 320 | 26.7 | -7.4 | -15.2 | 5.170 (1.75) | .047 (.030) |
| Right Amygdala | R | Insula (m)(-) | 320 | 41.1 | -14.1 | -8 | 5.640 (0.68) | .028 (.008) |
| | L | Amygdala (-) | 192 | -24.7 | -2.1 | -12 | 6.016 (.797) | .024 (.008) |
| | L | Insula (a/m)(-) | 1472 | -36.1 | -1.3 | 10.3 | 6.248 (3.26) | .040 (.035) |
| | B | Subgenual ACC | 1088 | -1.5 | 14.8 | -8.9 | 6.616 (2.74) | .033 (.037) |

Cluster coordinates and anatomical areas are for cluster center of mass as defined by Talairach stereotactic space; Negative (-) signs following anatomical area indicate reduced connectivity; Descriptors for ACC and insula clusters do not reflect stereotactic distinctions, but are estimates based upon the relative location of activation on the group map;

* Voxelwise statistics are presented with education covaried out; ROI=region of interest; WB=whole brain; m=middle insula; a=anterior insula; p=posterior insula.